A Lumped Element Modeling Schema for Metabotropic Signaling in Neurons

Richard B. Wells

MRC Institute, The University of Idaho

Abstract: A lumped element modeling schema is presented that can be usefully applied to modeling and analysis of metabotropic processes affecting the signal processing properties of neurons. The schema is easily applied to qualitative models of such biochemical processes and facilitates the development of differential equation descriptions. The state variables within the model are applicable to augmenting and extending Hodgkin-Huxley-like models (H-H models) of neuron dynamics.

I. Introduction

There is something to be said in favor of having a general and versatile modeling schema for particle accumulation, transport, chemical reaction, and storage in the cell. A general schema is an aid for transforming qualitative models into quantitative ones and for developing relationships descriptive of more complex physiological processes. After all, if the Hodgkin-Huxley schema is useful in part because it provides a guide for dealing with the complexities of voltage-gated-channel (VGC) and ligand-gate-channel (LGC) signaling, is it not also likely that a similar schema will prove useful for dealing with cellular biochemical signaling processes?

In this paper we resurrect and adapt to our purposes a modeling schema originally developed by Linvill [Linvill and Gibbons, 1961, pp. 17-48] and extend it to application in neuroscience. The Linvill model was developed to represent carrier transport, storage, and generation-recombination phenomena in semiconductors in terms of carrier densities and current flows. This method has not previously been applied to biological signaling processing models. After all, the neuron is not a transistor or a diode. Nonetheless, with only a few minor adaptations of the Linvill model, one can apply it as a schema for representing particle flux and concentration in the cell. This section introduces the basic modeling elements and their mathematical description. The next sections illustrate some of its potential applications.

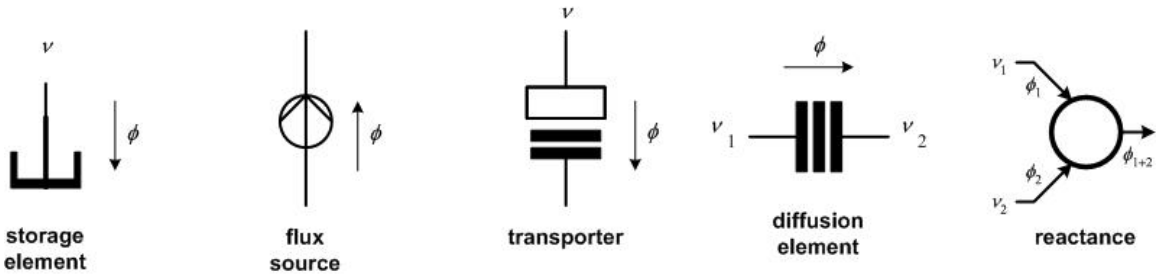

Figure 1: The five basic network elements of the Linvill modeling schema.

The Linvill modeling schema allows us to represent the model as a network of elements, each of which is characterized by a specific element law. Figure 1 illustrates the five basic Linvill network elements. Ion or molecule concentration is denoted by the symbol v. Ion or molecule flux is denoted by the symbol ϕ. Flux is positive in the direction denoted by the arrows. Particle (ion or molecule) motion in space is formally describable in terms of partial differential equations with boundary conditions. While such a description is mathematically rigorous and precise, it is also rather cumbersome and computationally difficult to deal with in all but the simplest cases of physical geometries. This issue is often overcome in the various sciences through the introduction of the lumped element approximation. For example, electric and magnetic phenomena are rigorously described by Maxwell's equations, a set of partial differential equations. Circuit theory is the lumped element approximation of these equations, applicable when electromagnetic radiation (a consequence of Maxwell's equations) is not an important factor. Similarly, the Linvill model is a lumped element approximation to a partial differential equation description of particle transport, storage, chemical reaction and accumulation processes.

The storage element ("storance") represents the accumulation of particles of a specific type in a region due to influx from some other location or source. Its v-ϕ relationship is based on the mathematical form of the divergence theorem. The element law merely states that the net influx of particles into the storage element is proportional to the time rate of change of concentration,

$$C\frac{dv}{dt} \stackrel{\Delta}{=} C\dot{v} = \phi \qquad (1)$$

Dimensional analysis shows C has units of volume. C reflects the fact that a region of greater volume builds up particle concentration less rapidly than a region of smaller volume for the same amount of flux. We may at once note the similarity between (1) and the element law for a capacitor in circuit theory. ϕ is analogous to electric current and v is analogous to voltage. There are, however, limits to this electric circuit analogy. The accumulation of v in a storage element does not induce the accumulation of some other particle elsewhere (no equivalent to charge on one plate of a capacitor inducing the opposite charge on the other plate), and there is nothing analogous to the displacement current through a capacitor, which is a consequence of Maxwell's equations. Likewise, there is no "Kirchhoff's voltage law" for this network. Particle flux is not required to flow in a closed circuit path, hence the model is a network model rather than a circuit model. Particle conservation, however, is required for the first four network elements because only the reactance element represents a chemical reaction, e.g. $a + b \rightarrow c$.

The flux source element represents influx/efflux from some exterior source. The most common use for this element is to convert electric currents obtained from a H-H model to particle flux. The current I due to a flux ϕ of particles with valence z is simply $I = ze\phi$ when ϕ is expressed in particles per second. It is more convenient, however, to express flux in units such as moles/second. In this case we would write $I = zF\phi$, where F is Faraday's constant. If we have a current *density* – amperes per unit area – we replace flux by flux density. Letting $\beta = 1/zF$ we obtain the element law as $\phi = \beta \cdot I$ with I in amperes and β in moles/coulomb. For $z = 1$, β is numerically equal to $10.3643 \cdot 10^{-6}$ moles/coulomb. Note that the sign of the valence is irrelevant to flux (since this is merely the sign of the electric charge carried). Therefore if one is modeling the flux of a negative-valence particle, the absolute value of z would be used.

The transporter symbol is a generalization of an element Linvill called a "combinance" [Linvill, 1961, pg. 25]. In his original model this element was used to model charge generation and recombination in semiconductors. That is a process by which bound charge is converted to

free charge and vice versa. The analog to this within the cell (not including chemical reactions that produce new compounds) are processes by which free particles are introduced or removed by various transport processes, such as the transport process by which free Ca^{2+} is removed from the cytoplasm and stored in the endoplasmic reticulum [Hille, 2001, pp. 269-273]. In effect, these are pumping processes in which the average flux is determined by the amount of particle transport per cycle of the pump and the concentration of the particle being transported. Thus, the simplest form of an element law for the transporter is the relationship

$$\phi = \rho \cdot \nu \qquad (2)$$

where ρ is an empirically-determined transport parameter with units of volume/second. Note that this expression is unidirectional. The concentration variable in (2) is placed at the "boxed" end of the network element, and whatever the concentration may be at the other terminal is irrelevant. The transporter does not represent a passive diffusion process. That dynamic is modeled by the fourth network element.

The diffusion element ("diffusance") represents particle flux due to concentration differences. Flux is positive in the direction from higher concentration to lower concentration. In its simplest form, the diffusance element law is merely

$$\phi = D \cdot (\nu_1 - \nu_2) \qquad (3)$$

where D is an empirically-determined parameter with units of volume/second.

If C, ρ, and D are represented by simple constants we have a linear model of transport and storage. Making these variables functions of ν, and possibly other variables, produces a nonlinear model. At our present state of knowledge of neural metabotropic physiology no nonlinear model of the neuron's internal processes is in widespread use and, consequently, most computational neuron modeling works have used linear models for most simple transport and storage processes. This does not mean such models are correct; it merely reflects the state of knowledge one has.

Using the first four elements we can construct network models of arbitrary complexity to

represent various transport and storage processes excepting those involving chemical reactions. Chemical reactions are modeled by the reactance element, which is discussed later in this paper. If it happens to be the case where we do not care what happens later to these reaction products, a derived element, called a reactor, combined with a storage element can suffice for representing the introduction or the removal of free particles. This is also illustrated later. The next section illustrates the application of this modeling schema to Ca^{2+} augmentation of the basic H-H model.

II. Simple Models of Ca^{2+} Processes in the Neuron

The simplest and most common model of Ca^{2+} buffering in the neuron represents the gross influx of Ca^{2+} from calcium channels and the removal of free Ca^{2+} from the cytoplasm by a transport process. Figure 2 illustrates the model network. The endoplasmic reticulum is regarded as having infinite volume and so the time rate of change of $[Ca^{2+}]$ at this node is zero. I_{Ca} is obtained from the electrical model of the neuron, and its numerical value from the Goldman-Hodgkin-Katz (GHK) current equation is negative or zero. Thus, the network of Figure 2 receives an influx of Ca^{2+} into node *v*. Summing the effluxes from this node, we obtain the dynamical equation

$$C\frac{dv}{dt} = -\rho \cdot v - \beta \cdot I_{Ca}(t) \ . \qquad (4)$$

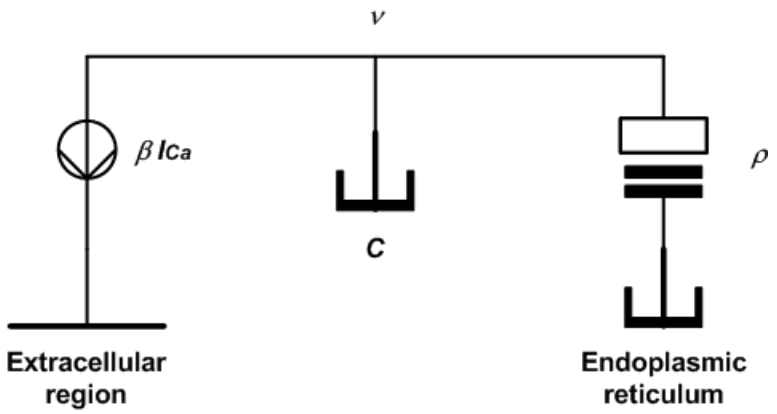

Figure 2: Simple model of free Ca^{2+} buffering. I_{Ca} is obtained from the electrical model of the neuron. Because its numerical value is negative, the Ca network receives a Ca^{2+} influx.

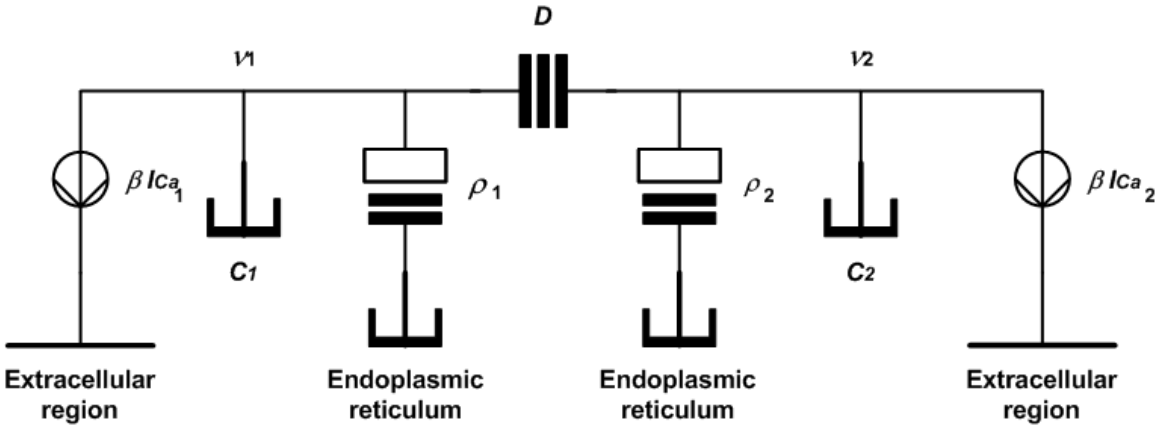

Figure 3: Two-compartment model of a Ca^{2+} network.

Most calcium buffering models incorporate a constraint that the minimum level of $[Ca^{2+}]_i$ is not allowed to fall below some minimum value $[Ca^{2+}]_{min}$. This is easily incorporated into the network of Figure 2 by adding a phenomenological "calcium leakage flux" in parallel with the calcium flux obtained from the electrical model. Setting the derivative in (4) to zero, we obtain for this leakage flux the numerical value $\beta \cdot I_{leak} = -\rho \cdot [Ca^{2+}]_{min}$. The direction of the arrow for this flux source is the same as that of the source shown in Figure 2.

McCormick and Huguenard [McCormick and Huguenard, 1992] argued that the literature on neuron physiology suggested HVA calcium channels, $I_{Ca(L)}$, and LVA T-current channels, $I_{Ca(T)}$, are probably located in different regions of the neuron. They used this argument to justify making their Ca^{2+}-dependent K^+ VGC element depend on the contribution to $[Ca^{2+}]$ from the L-current only. In their model they kept track of the individual contributions from $I_{Ca(L)}$ and $I_{Ca(T)}$ while still letting their GHK current model depend on the sum of the two components. In effect, their model is something like a two-compartment model of the calcium network, although not entirely rigorous in its formulation. A more formal representation of two-compartment modeling is illustrated in Figure 3. The schema is easily extended for representing any number of calcium compartments.

Summing the effluxes from each node and rearranging terms we obtain a system of two differential equations,

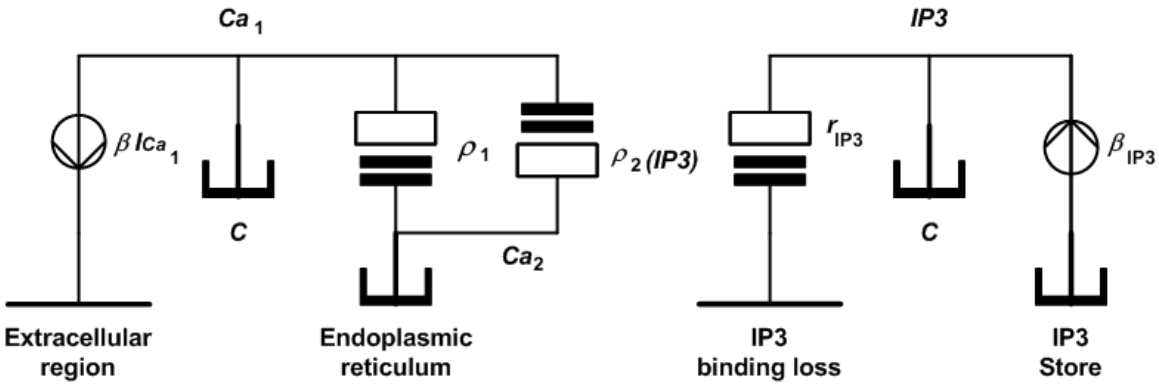

Figure 4: Simplified model of metabotropic-signal-induced calcium release.

$$\begin{bmatrix} dv_1/dt \\ dv_2/dt \end{bmatrix} = \begin{bmatrix} -(\rho_1 + D)/C_1 & D/C_1 \\ D/C_2 & -(\rho_2 + D)/C_2 \end{bmatrix} \begin{bmatrix} v_1 \\ v_2 \end{bmatrix} + \begin{bmatrix} -\beta_1/C_1 & 0 \\ 0 & -\beta_2/C_2 \end{bmatrix} \begin{bmatrix} I_{Ca_1} \\ I_{Ca_2} \end{bmatrix}. \quad (5)$$

As a final calcium example we will consider a metabotropic signaling process in which internal Ca^{2+} stores are released from the endoplasmic reticulum to become free Ca^{2+} in the cytoplasm. Figure 4 illustrates the model. This model is intended to illustrate the general ideas conveyed by qualitative models of this process. It should be noted that our present state of knowledge of the quantitative details of this process is incomplete and so the model presented here is to be regarded as conceptual but not an established accurate representation of this process.

The model contains two types of chemical concentrations, $[Ca^{2+}]_i$ represented on the left by node variable Ca_1, and cytoplasmic concentration of inositol triphosphate (IP_3) represented by node variable *IP3* on the right. Ca_2 represents the concentration of Ca^{2+} stored in the endoplasmic reticulum (ER). Typical concentrations of stored Ca^{2+} is typically greater than 100 μM under normal physiological conditions and likely reaches millimolar levels. The ER's supply of Ca^{2+} is by no means unlimited, but for normal signal processing functions we can regard the volume C_{ER} as effectively infinite so that concentration Ca_2 may be regarded as constant. We will also assume flux source $\beta \cdot I_{Ca1}$ includes a leakage flux that maintains the minimum level of Ca_1 at its resting concentration level (on the order of 50 to 100 nM). Transporter ρ_1 is the same as described

previously. We will come back to transporter ρ_2 momentarily.

In the absence of synaptic metabotropic signaling, IP_3 is normally bound in the cytoplasmic membrane wall. It is liberated by the action of a membrane-spanning G-protein acting as a molecular switch to turn on the production of second messenger chemicals, IP_3 in this case. Flux source β_{IP3} models the generation of free IP_3 by this mechanism. The units of β_{IP3} are flux (moles per second). Free IP_3 moves to the ER and binds with Ca-release channels in the membrane of the ER. As IP_3 again becomes bound by this process, it depletes the pool of free IP_3 and we can represent the rate of this depletion using transporter r_{IP3}. Thus, the concentration *IP3* is described by[1]

$$C\frac{dIP3(t)}{dt} = -r_{IP3}\cdot IP3(t) + \beta_{IP3}\,. \qquad (6)$$

Transporter $\rho_2(IP3)$ represents the influx of free Ca^{2+} due to the opening of the calcium-release channels in the ER. The kinetics of this process are complicated [Moraru et al., 1999], but we can pose a few likely-seeming approximations. First, since the Ca^{2+} influx is zero in the absence of IP_3, the simplest plausible model for this effect is to presume the influx is proportional to $IP3(t)$. This assumption is analogous to that used in modeling calcium buffering in (4). Second, it is known that the opening probability, π_o, of the ER's calcium-release channels is strongly affected by the concentration level of cytoplasmic free calcium, Ca_1 [Bezprozvanny et al., 1991], [Finch, 1991], [Moraru et al., 1999]. Bezprozvanny et al. report a bell-shaped curve function for release probability vs. $[Ca^{2+}]_i$ that reaches a peak of $\pi_o = 1$ at around $Ca_1 = 0.2$ μM. The bell shape of the π_o dependency shows up on a logarithm plot of $[Ca^{2+}]_i$, i.e. the $\pi_o = 0.5$ points on the curve occur at approximately 0.075 μM and 0.55 μM [Bezprozvanny et al., 1991]. Bezprozvanny et al. report the fitted dependency as

[1] There are other dynamics we are not representing accurately in this simplified model. For example, IP_3 does not remain indefinitely bound to the calcium-release channels, and this model depicts neither how long IP_3 remains bound (thus activating the channel) nor what happens to it later. An understanding of these additional dynamics is necessary for a complete and accurate model of this process [Moraru et al., 1999]. The example given here is intended to merely illustrate an application of the Linvill model.

$$\pi_o = \pi_s \frac{Ca_1^n \cdot k_1^n}{\left(Ca_1^n + k_2^n\right)\cdot\left(Ca_1^n + k_1^n\right)} \qquad (7)$$

where π_s is a scale factor chosen to make π_o equal to 1 at Ca_1 = 0.2 μM, n = 1.8, $k_1 = k_2$ = 0.2 μM. Figure 5 graphs (7) as a function of calcium concentration Ca_1.

Taking these factors into account, we would write the transporter element law as

$$\rho_2 = \pi_o(Ca_1)\cdot \rho_{max} \cdot IP3(t); \quad \phi_2 = \rho_2 \cdot Ca_2 .$$

One noteworthy property of this system is the following. For concentrations Ca_1 less than about 0.2 μM, π_o is an *increasing* function of Ca_1, and thus there is a positive-feedback effect taking place inducing a strong rise in free cytoplasmic calcium. Above this level, π_o is a decreasing function of Ca_1, and so the total rise in free calcium is self-inhibited by the kinetics of the release probability. This has been known to produce oscillations in the concentration levels of free $[Ca^{2+}]_i$ in response to metabotropic signaling. This results in calcium-mediated modulation of ionotropic potassium currents [Hille, et al., 1995]. The oscillations are spike-like and very slow, with period on the order of 12 to 20 seconds per spike for the case where IP_3 is produced in response to metabotropic action by the neuropeptide GnRH (gonadotropin-releasing hormone). Calcium spikes with peaks in the range of about 1.5 to 2.5 μM have been observed.

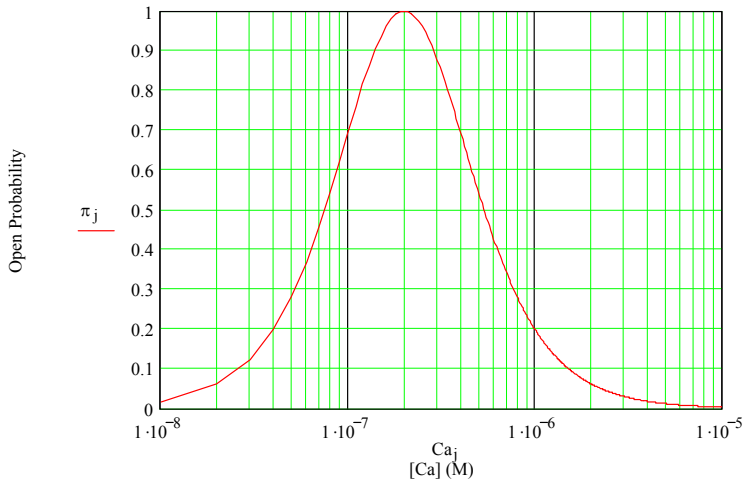

Figure 5: Empirical curve fit to calcium release channel open probability.

Summing effluxes from the Ca_1 node and incorporating (6) gives us the system of first order differential equations

$$\begin{bmatrix} dCa_1/dt \\ dIP3/dt \end{bmatrix} = \begin{bmatrix} -\rho_1/C & 0 \\ 0 & -r_{\mathrm{IP3}}/C \end{bmatrix} \cdot \begin{bmatrix} Ca_1 \\ IP3 \end{bmatrix} + \begin{bmatrix} \rho_2/C & -\beta/C & 0 \\ 0 & 0 & 1/C \end{bmatrix} \cdot \begin{bmatrix} Ca_2 \\ I_{Ca_1} \\ \beta_{\mathrm{IP3}} \end{bmatrix}. \quad (8)$$

Although the equations in (8) appear to be uncoupled, in fact they are not. *IP3* couples into the first equation through ρ_2.

An additional consideration not incorporated into this simplified model would account for loss of free calcium through binding with the calcium-releasing channels depicted by ρ_2. The kinetics model of [Moraru et al., 1999] assumes two Ca^{2+} ions and four IP_3 molecules participate in each binding event at the receptor site for the calcium-releasing channels. This, however, could be taken into account in an approximate fashion by the numerical value assigned to ρ_2. More important is the absence in the simplified model of a time-dependent rate process description for transporters ρ_2 and r_{IP3}. In the simplest case we would have at least one additional differential equation, possibly similar to a rate process model such as is used in the Hodgkin-Huxley schema, capturing the opening- and closing-kinetics of the calcium releasing channels. Such a process would affect the time-dependencies of both ρ_2 and r_{IP3}. Judging from the findings reported in [Moraru et al., 1999], time constants for such a process are on the order of a few milliseconds.

As a final note, the model just presented is a very simplified representation of these dynamics. Much more elegant treatments based on diffusion theory and partial differential equation models have been formulated [Schutter and Smolen, 1998]. A lumped approximation for this type of model would require the model of Figure 4 to be turned into a multi-compartment model.

III. The Reactance Element in the Linvill Modeling Schema

It is well known that metabotropic signaling plays an important control function in biological signal processing. Metabotropic signaling occurs by means of cascade biochemical reactions in

the cell that alter basic properties in the flow of ionotropic signaling pathways. The reactance element is the element in the Linvill network modeling schema that models chemical reactions.

The basic element shown in figure 1 has two inputs and one output. The reactance can be easily extended to take into account more input reactants and/or to produce more than one reaction product. In this section the action of the reactance element is illustrated for the simplest case of two inputs and one output as shown in figure 6 below.

Consider the case of a simple chemical reaction in terms of concentrations of substances, e.g.,

$$2\nu_1 + \nu_2 \rightarrow 2\nu_3 .$$

We assume all three substances are co-located within the same volume within the cell. Because the substances represent different chemical species, three storance elements are required, as shown in the figure. Noting the flux directions indicated in the figure and applying the storance element law, we have

$$\phi_1 = -C\dot{\nu}_1 ; \quad \phi_2 = -C\dot{\nu}_2 ; \quad \phi_3 = C\dot{\nu}_3 .$$

Noting the stoichiometric coefficients in the chemical reaction equation above, we also have

$$\phi_1 = \phi_3 ; \quad \phi_2 = 0.5 \cdot \phi_1 .$$

Chemical reaction kinetics are governed by the mole balance equation [Fogler, 1999, pp. 6-16] and by the form of the reaction rate equation. In general, reaction rate equations are algebraic equations, rather than differential equations, and are frequently deduced from experimental data. Generally, a reaction rate equation would be of the form $\phi_i = f_i(\nu_1, \nu_2, \nu_3)$ where f_i is some algebraic function of the concentrations of the three substances involved in the reaction [Fogler, 1999, pp. 73-113]. For purposes of our present example, we will assume the reaction is governed by the simplest form of reaction rate expression, namely the second order reaction,

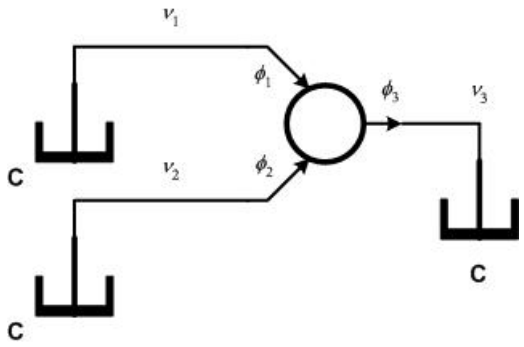

Figure 6: Linvill reactance element example.

$$C\dot{v}_1 = -\alpha \cdot v_1 \cdot v_2$$
$$C\dot{v}_2 = -0.5 \cdot \alpha \cdot v_1 \cdot v_2 \quad .$$
$$C\dot{v}_3 = \alpha \cdot v_1 \cdot v_2$$

Here α is a non-negative proportionality constant for the reaction rate. Note that the simple second order reaction model used here makes the system of differential equations describing the network a nonlinear system model even if all the other Linvill elements in the network are described by linear differential equations.

In a more complex network than the one depicted in figure 6, the first two equations above merely enter in as terms in the differential equation for nodes 1 and 2, respectively, and account for the disappearance of substances v_1 and v_2 that occurs during the chemical reaction. The third differential equation above is a new term introduced into the overall set of network equations by the reactance element. In other words, a reactance element having only a single output product introduces one new differential equation into the system model, namely that of the reaction product. In general, one new differential equation is introduced for each output product. The relative amounts of flux associated with each substance is determined from the stoichiometry of the chemical reaction [Fogler, 1999, pp. 33-35].

IV. The Derived Reactor Element in the Linvill Modeling Schema

In some important biochemical reactions one of the reactants, let us say v_2 for example, may merely act as a catalyst and take no other part in the reaction. The simplest example would be the case where v_1 is an inactive isomer and v_3 is an active isomer form of the same substance. In this

case we would have $\phi_2 = 0$ because catalyst ν_2 is neither increased nor decreased by the reaction it catalyzes. Often the reaction rate in such a case might involve a first-order reaction, $f = \alpha \cdot \nu_2$, in the expressions for ϕ_1 and ϕ_3. In such simple cases as this, the Linvill network can often be simplified by the introduction of a sixth element, called a reactor, which is mathematically identical to the transporter element in figure 1 except that the substances represented at the two terminals are different substances. The reactor element can be regarded as a special case of a one-input/one-output reactance.

At the present time, it is the unfortunate case that the research literature reporting the findings of biochemical studies in neuroscience frequently omit findings regarding the specific reaction rate kinetics of the biochemical reactions being studied. It can be hoped that the introduction of the Linvill modeling schema may help to change this situation. In the absence of reported experimental facts, the mathematical modeler can only have recourse to phenomenological guesses of what form of reaction rate equation f might be involved in a particular system under study. Quantitative results from such modeling work can serve to pose questions to other researchers that subsequent experiments can confirm or refute. One example of this is a recent work by Ramirez on modeling of monoclonal antibodies in the treatment of methamphetamine addiction [Ramirez, 2008].

It has been well established that phosphorylation/dephosphorylation is an important, and perhaps the primary, mechanism for regulating receptor sensitivity and modulating ion channel dynamics [Huganir and Greengard, 1990], [Levitan, 1994]. While physiologists, molecular biologists, and neurochemists have long been aware of the importance of phosphorylation/dephosphorylation in the regulation of neuronal activity, this has not yet been widely recognized by neural network theorists in the form of neural network models that include it in their structures. Of the major schools of neural network theory, only adaptive resonance theory has so far incorporated mathematics to give a well-organized account for the modulation phenomena, albeit this

accounting is high-level, abstract, and quite indirect. Yet most of the major subsystems in the brain that signal by means of metabotropic messengers have widespread targets across large regions of the neocortex and other cerebral structures. Because these modulating signals work through phosphorylation and dephosphorylation, this lack of attention by neural network theorists is difficult to justify.

Not surprisingly, the kinetics of phosphorylation are different for the many different kinds of kinases. We will not delve into the fine details of the biochemistry involved here, mainly because there are so many but also because this is a topic for specialists. Some excellent reviews are available describing PKA [Francis and Corbin, 1994], PKC [Tanaka and Nishizuka, 1994], the CaM kinases [Hanson and Schulman, 1992], and the receptor tyrosine kinases [Fantl et al., 1993]. In this paper the focus will be given to common features found in the processes of the phosphorylation/dephosphorylation cycle.

A kinase exhibits (at least) two states, called *active* and *inactive*. A kinase in the active state produces phosphorylation of its target substrate protein. Phosphorylation is often ATP-dependent, and it produces compounds which are highly reactive in water with other organic molecules in the presence of appropriate enzymes. An inactive kinase is one in a configuration where it does not act as such a catalyst.

Second messengers cause a kinase to enter the active state. Other factors in the cell's chemical milieu, not all of which are particularly well understood, return a kinase to its inactive (basal) state. In addition to phosphorylating substrate proteins, some kinases have the ability to phosphorylate themselves; this is called autophosphorylation. A kinase in this state remains at least partially active and is returned to the inactive state through the action of a phosphatase. Let S_0 denote the inactive state of a kinase. Let S_1 represent the normal active state of the kinase, and let S_2 represent the autophosphorylated active state.

By introducing a new element in the Linvill modeling schema, called the reactor, we can represent the process just described. The simplest feasible representation is shown in Figure 7.

The flux law for a reactor element, R, is identical to that of a transporter, T, except for its physical interpretation. Unlike transporter flux, which represents the active transport of a substance from one location to another, reactor flux represents the loss of concentration of a substance, [X], due to a chemical reaction or a change in chemical state involving substance X. The reactor flux is given by

$$\phi_R = R \cdot [X].$$

In general, the value of R will be a function of the concentration of some other substance, [Y], with which X is undergoing chemical reaction or which causes the change in chemical state of X. For example, reactor R_2 in figure 7 will be a function of the second messenger concentration [m]. Similarly, reactor R_m in the figure will be a function of [S_0], the concentration of inactive secondary effector kinase acted upon by second messenger m. Thus, the two Linvill networks in the figure are non-linearly coupled through the co-dependencies of the reactor elements. The sign convention for reactor flux is the same as that of the transporter element. For example, the differential equation describing node [S_2] in the network is

$$C \cdot \frac{d[S_2]}{dt} = R_3 \cdot [S_1] - R_4 \cdot [S_2].$$

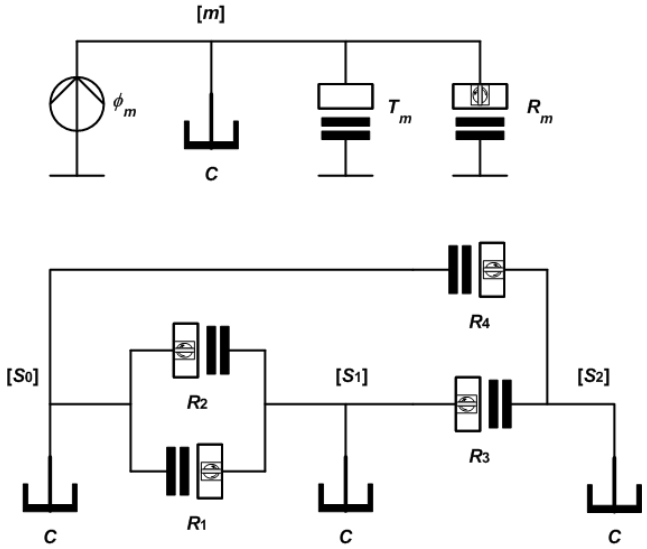

Figure 7: A simple Linvill schema for modeling inactive, active, and partially active kinase activated by a second messenger, *m*.

In general there will be one first-order differential equation for each storance element in the network. Applying the element laws to the network of figure 7 we obtain the coupled system of equations

$$\begin{bmatrix} d[m]/dt \\ d[S_0]/dt \\ d[S_1]/dt \\ d[S_2]/dt \end{bmatrix} = \begin{bmatrix} -(T_m + R_m)/C & 0 & 0 & 0 \\ 0 & -R_2/C & R_1/C & R_4/C \\ 0 & R_2/C & -(R_1 + R_3)/C & 0 \\ 0 & 0 & R_3/C & -R_4/C \end{bmatrix} \cdot \begin{bmatrix} [m] \\ [S_0] \\ [S_1] \\ [S_2] \end{bmatrix} + \begin{bmatrix} 1/C \\ 0 \\ 0 \\ 0 \end{bmatrix} \cdot \phi_m \, .$$

Here flux ϕ_m represents the production of second messenger chemical *m*. It should be observed that terms such as *C*/*R* and *C*/*T* have units of time constants and their inverses have units of transport or reaction rates. Therefore, owing to the general form of the system of equations, the number of parameters to be determined experimentally is generally fewer than the number of network elements because determination of time or rate constants (which in general will not actually be "constants"; the H-H model is likewise so) is sufficient to determine the numerical parameters of the dynamical equation.

Many kinases exhibit a threshold effect for their activation by second messengers. This implies that the dependency of R_2 on [*m*] is likely to follow a Boltzmann function or a function similar in general form to a Boltzmann function. At least some second messengers (such as cAMP) are known to be able to reach any part of a mammalian cell. In the case of cAMP, this can be accomplished in 100 ms. This omnipresent spread of second messengers might be true for most of the major second messengers in the neuron. It is therefore a reasonable speculation that the rate of activation of the messenger's target kinases is a function of messenger concentration, [*m*], which is in turn a function of its production rate by the first effector (represented by ϕ_m in figure 7). Similarly, it is a reasonable speculation that the rate of phosphorylation of target substrate proteins (e.g. an ionotropic channel protein) is a function of the concentrations of active second effectors ([S_1] and [S_2] in figure 7) and of the concentration of non-phosphorylated target proteins (e.g. the number of such proteins in the neuron divided by the aqueous volume of the

cell). Modeling this requires that a third subnetwork, along the same lines as the lower subnetwork in figure 7, be added to the total network model.

V. Discussion

The principal protein kinases are widely expressed throughout the central nervous system. Often they are heavily concentrated in the postsynaptic density. Because these membrane spanning proteins are target substrate proteins for active kinases, this localization is further evidence for how the modulatory role of these kinases is realized in biological signal processing.

At the present state of signal processing model theory for the neuron, there are many important factors for which we are not yet in possession of quantitative data needed to develop an accurate model. No doubt a large of amount of this information lies buried in the biochemistry and organic chemistry literature, e.g. [Buxbaum and Dudai, 1989], expressed there in the language of the chemist rather than that of the neuroscientist. No doubt, too, some of this information is still entirely unknown, the relevant modeling research question not having yet been posed. This is an under-recognized research field for computational neuroscience and biological signal processing. There is very clear evidence that for many of the important kinases their activity level (which one can assess by examining the rates at which they phosphorylate their targets) is more complex than being merely binary or ternary (as figure 7 might suggest). Reports in the bio-chemistry literature indicate that the activity levels of the major kinases is dependent upon levels of ATP concentration and probably other factors as well. Accounting for this clearly requires a more complex network model than the example given above. Indeed, the need for this accounting is one reason why a method of lumped-element representation of the process is useful and important for understanding the modulation processes of the neuron.

The experimentally observed fact that many of the major protein kinases, especially PKC and CaM, exhibit autophosphorylation, and thus remain partially active even after concentration levels of their second messengers decline, has been a source of great scientific interest. There is a good deal of speculation that autophosphorylation of the kinases is a memory mechanism for the

neuron [Schwartz and Greenberg, 1987]. This appears to be an undeniable fact in the case of elastic modulation, a form of short-term memory for the neuron. Additional evidence suggests that some kinases, particularly CaM and presynaptic PKC, may also support plastic (that is, irreversible) modulation of synaptic efficacy. Presently, this putative role is still somewhat speculative, but it is receiving a great deal of attention and one can reasonably expect the future to bring further clarification to this possibility. It is clear that, as a flexible modeling schema, the Linvill modeling schema has the potential to play an important quantitative role in this research.

The secondary effectors primarily exert their effects through phosphorylation of their target substrate proteins. The phosphorylation process is accompanied by another regulatory process, namely the process of dephosphorylation. Phosphorylation of the substrate protein can, depending on the kinase involved and the particulars of the target protein, work either to sensitive or to desensitize the response of the channel protein in responding to neurotransmitters. In some cases it can open a normally-closed channel; in others it can close a normally-open channel. One model of this effect, although disputed by some researchers, holds that phosphorylation of channel proteins can be represented by introducing the idea of an effective density of channel proteins in the synapse. In this phenomenological model, the effect of phosphorylation is looked upon as having the same effect as increasing (or decreasing) the number of receptors on the postsynaptic side of the synapse. AMPA receptors are often treated this way, although there seems to be no strong reason to exclude the other ionotropic receptors from being looked at in this way. However, as already noted, other researchers take issue with this model of cell response to the secondary effectors, and the matter seems to be far from settled on the physiology level. Computational neuroscientists, on the other hand, have been quick to adopt this model of channel sensitization/desensitization. Better quantitative modeling can be expected to help bring the issue to a better determination.

Presynaptic protein kinases might possibly target synaptic vesicle membranes or other structures within the synaptic terminal and thereby effect a change in the efficacy of

neurotransmitter exocytosis. This is presently regarded as rather speculative and is often accompanied by the hypothesis that membrane-permeable retrograde messengers such as NO must also be involved in such a process. NO is a byproduct of the action of the arachidonic acid (AA) process; the DAG-PKC second messenger process is thought to produce AA as a divergence byproduct. Putative mechanisms such as these are easily added to theoretical models by means of the appropriate Linvill network.

Dephosphorylation is the removal of the phosphate group from the target protein. It is also the mechanism by which autophosphorylated protein kinases become inactive once again. Dephosphorylation is produced by enzymes called phosphoprotein phosphatases. Whatever the cell response to the secondary effector was, dephosphorylation terminates the effect. Reactor R_4 in figure 7, which represents dephosphorylation of an autophosphorylated kinase, is an example of how the Linvill modeling schema can represent of this effect. A large value of R_4 (or, equivalently, R_4/C) represents rapid dephosphorylation; a small value represents slow dephosphorylation.

Dephosphorylation can itself be regulated by metabotropic mechanisms. One well-studied case is that of phosphorylation of K^+ channels by the action of PKA [Siegelbaum et al., 2000]. In this case, a K^+ channel opened by phosphorylation is dephosphorylated and closed by the action of phosphoprotein phosphatase-1. However, the action of this enzyme is regulated by another protein, inhibitor-1. Inhibitor-1 is phosphorylated by the action of PKA, and in this state it inhibits the action of phosphoprotein phosphatase-1. Here is one example of how one metabotropic signaling cascade can diverge (PKA inhibiting dephosphorylation, while at the same time producing it in the K^+ channel). Inhibitor-1 is dephosphorylated by the action of Ca^{2+}, which activates the phosphatase calcineurin that in turn dephosphorylates inhibitor-1. A similar process has been reported for regulating phosphorylation/dephosphorylation of NMDA receptors [Halpain et al., 1990]. This one involves inactivation of the inhibitor DARPP-32 by CaM and activation of DARPP-32 by PKA produced from elevated cAMP levels stimulated by dopamine

signaling.

Each of these actions just described can be approximated by adding additional Linvill networks to those depicted in figure 7. In the case of targeted channel proteins, if one adopts the effective-density model the relevant concentrations would be concentrations ν_p of phosphorylated channels and ν_d of dephosphorylated channels. Reactor elements would be used to model the kinetics of the phosphorylation/dephosphorylation process in terms of concentrations of various active secondary effectors. Modeling of dephosphorylation would involve networks, similar to the lower network in figure 7, modeling the concentrations of inhibited and uninhibited phosphatases, calcineurin, etc.

Perhaps the principal significance of all of this is the following. The Linvill modeling schema provides a more or less straightforward way for the investigator to proceed from a qualitative model of putative mechanisms, such as are common in neurobiology, to quantitative mathematical models of the hypothesis. This process not only brings into prominence the key factors required to obtain specific predictions and implications of a theory, but also points toward new experiments addressed to the purpose of discovering quantitative information about these mechanisms. In this way, models assist in the logical progression of research programs and are a source of significant research questions and aims. Furthermore, one need not be a highly trained mathematician in order to be able to propose such mathematical models. Ramirez, for example, had no more than a basic knowledge of calculus and yet was able to produce a interesting and fairly accurate model of monoclonal antibody kinetics from a starting point of merely qualitative information regarding the putative action of these antibodies in treating methamphetamine addiction [Ramirez, 2008].

In conclusion, this paper has presented the Linvill modeling schema as an efficient approach for the development of quantitative models and theories in biochemical cascade reaction signaling (metabotropic signaling). It is proposed that this methodology holds much research promise.

References

Bezprozvanny, I., J. Watras and B.E. Ehrlich, "Bell-shaped calcium-response curves of Ins(1,4,5)P_3- and calcium-gated channels from endoplasmic reticulum of cerebellum," *Nature (Lond.)*, 351: 751-754, 1991.

Buxbaum, Daniel J. and Yadin Dudai, "A quantitative model for the kinetics of cAMP-dependent protein kinase (type II) activity," *J. Biol. Chem.*, vol. 264, no. 16, June 5, 1989, pp. 9344-9351.

Fantl, Wendy J., Daniel E. Johnson, and Lewis T. Williams, "Signalling by receptor tyrosine kinases," *Annu. Rev. Biochem.*, 62: 453-481, 1993.

E.A. Finch, E.A., T.J. Turner and S.M. Goldin, "Calcium as a coagonist of inositol 1,4,5-triphosphate-induced calcium release," *Science*, 252: 443-446, 1991.

Fogler, H. Scott, *Elements of Chemical Reaction Engineering,* 3rd ed., Upper Saddle River, NJ: Prentice-Hall, 1999.

Francis, Sharron H. and Jackie D. Corbin, "Structure and function of cyclic nucleotide-dependent protein kinases," *Annu. Rev. Physiol.*, 56: 237-272, 1994.

Halpain, Shelley, Jean-Antoine Girault, and Paul Greengard, "Activation of NMDA receptors induces dephosphorylation of DARPP-32 in rat striatal slices," *Nature*, vol. 343, pp. 369-372, Jan., 1990.

Hanson, Phyllis I. and Howard Schulman, "Neuronal Ca^{2+}/calmodulin-dependent protein kinases," *Annu. Rev. Biochem.*, 61: 559-601, 1992.

Hille, B., A. Tse, F.W. Tse and M.M. Bosma, "Signaling mechanisms during the response of pituitary gonadotropes to GnRH," *Recent Prog. Horm. Res.*, 50: 75-95, 1995.

Hille, Bertil, *Ion Channels of Excitable Membranes*, 3rd ed. Sunderland, MA: Sinauer Associates, 2001.

Huganir, Richard L. and Paul Greengard, "Regulation of neurotransmitter receptor desensitization by protein phosphorylation," *Neuron*, 5: 555-567, Nov., 1990.

Levitan, Irwin B., "Modulation of ion channels by protein phosphorylation and dephosphorylation," *Annu. Rev. Physiol.*, 56: 193-212, 1994.

J.G. Linvill, J.G. and J.F. Gibbons, *Transistors and Active Circuits*, NY: McGraw-Hill, 1961.

McCormick, D.A. and J.R. Huguenard, "A model of the electrophysiological properties of thala-mocortical relay neurons," *J. Neurophysiol.*, 68: 1384-1400, 1992.

Moraru, I.I., E.J. Kaftan, B.E. Ehrlich and J. Watras, "Regulation of type 1 inositol 1,4,5-triphosphaste-gated calcium channels by $InsP_3$ and calcium: Simulation of single channel kinetics based on ligand binding and electrophysiological analysis," *J. Gen. Physiol.*, 113: 837-849, 1999.

Ramirez, Sarahi, "Modeling the effect of monoclonal antibodies in the treatment of methamphetamine addiction using the Linvill modeling schema," poster presentation, Sigma Xi Annual Meeting and Student Research Competition, Washington, DC, Nov. 21, 2008.

Schutter, Erik De and Paul Smolen, "Calcium dynamics in large neuronal models," in *Methods in Neuronal Modeling*, 2nd ed., C. Koch and I. Segev (Eds.), Cambridge, MA: The MIT Press, 1998, pp. 211-250.

Schwartz, James H. and Steven M. Greenberg, "Molecular mechanisms for memory: Second-messenger induced modifications of protein kinases in nerve cells," *Annu. Rev. Neurosci.*, 10: 459-476, 1987.

Siegelbaum, Steven A., James H. Schwartz, and Eric R. Kandel, "Modulation of synaptic transmission: Second messengers", in *Principles of Neural Science*, 4th ed. (Eric R. Kandel, James H. Schwartz, and Thomas M. Jessell, Eds.), NY: McGraw-Hill, 2000, pp. 229-252

Tanaka, Chikako and Yasutomi Nishizuka, "The protein kinase C family for neuronal signaling," *Annu. Rev. Neurosci.*, 17: 551-567, 1994.